THE JOURNAL OF PHYSICAL CHEMISTRY A

Article

pubs.acs.org/JPCA

Tropospheric Aqueous-Phase Oxidation of Isoprene-Derived Dihydroxycarbonyl Compounds

Published as part of The Journal of Physical Chemistry virtual special issue "Veronica Vaida Festschrift".

Tobias Otto, Bastian Stieger, Peter Mettke, and Hartmut Herrmann*

Leibniz Institute for Tropospheric Research (TROPOS), Atmospheric Chemistry Department (ACD), Permoserstrasse 15, 04318 Leipzig, Germany

Supporting Information

ABSTRACT: The dihydroxycarbonyls 3,4-dihydroxy-2-butanone (DHBO) and 2,3-dihydroxy-2-methylpropanal (DHMP) formed from isoprene oxidation products in the atmospheric gas phase under low-NO conditions can be expected to form aqSOA in the tropospheric aqueous phase because of their solubility. In the present study, DHBO and DHMP were investigated concerning their radical-driven aqueous-phase oxidation reaction kinetics. For DHBO and DHMP the following rate constants at 298 K are reported: $k(OH + DHBO) = (1.0 \pm 0.1) \times 10^9$ L mol^{-1} s^{-1}, $k(NO_3 + DHBO) = (2.6 \pm 1.6) \times 10^6$ L mol^{-1} s^{-1}, $k(SO_4^- + DHBO) = (2.3 \pm 0.2) \times 10^7$ L mol^{-1} s^{-1}, $k(OH + DHMP) = (1.2 \pm 0.1) \times 10^9$ L mol^{-1} s^{-1}, k $(NO_3 + DHMP) = (7.9 \pm 0.7) \times 10^6$ L mol^{-1} s^{-1}, $k(SO_4^- + DHMP) = (3.3 \pm 0.2) \times 10^7$ L mol^{-1} s^{-1}, together with their respective temperature dependences. The product studies of both DHBO and DHMP revealed hydroxydicarbonyls, short chain carbonyls, and carboxylic acids, such as hydroxyacetone, methylglyoxal, and lactic and pyruvic acid as oxidation products with single yields up to 25%. The achieved carbon balance was 75% for DHBO and 67% for DHMP. An aqueous-phase oxidation scheme for both DHBO and DHMP was developed on the basis of the experimental findings to show their potential to contribute to the aqSOA formation. It can be expected that the main contribution to aqSOA occurs via acid formation while other short-chain oxidation products are expected to back-partition into the gas phase to undergo further oxidation there.

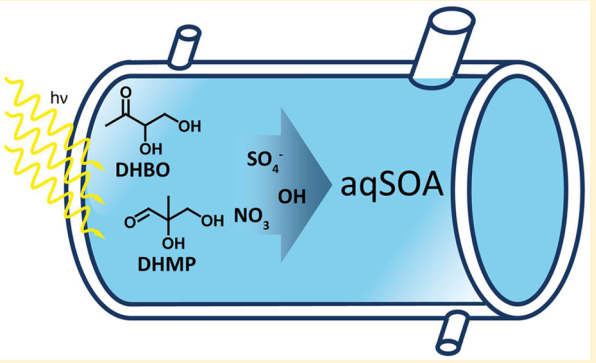

INTRODUCTION

The global annual emissions of biogenic volatile organic compounds is estimated to be 1007 Tg y^{-1}.[1] Among these, isoprene is the most emitted single compound within with a source strength of about 594 ± 34 Tg y^{-1}.[2] The oxidation chemistry of isoprene strongly affects the atmosphere's oxidation budget[3−5] and the formation of organic aerosol mass.[6−23] In regions influenced by anthropogenic activities the gas-phase oxidation of isoprene (high NO conditions) leads to the formation of C_5 hydroxynitrates (yield approximately 12%),[24−26] C_5 hydroxycarbonyls (yield approximately 20%),[26−29] C_4 hydroxycarbonyls (yield approximately 3%),[26,28,30,31] methacrolein and methyl vinyl ketone (yield approximately 30% as sum of methacrolein and methyl vinyl ketone),[26,30,32−34] methylglyoxal (yield approximately 4%),[26,28,30,31] glyoxal (yield approximately 2%),[26,28,30,31] glycolaldehyde (yield approximately 3%),[26,28,30,31] hydroxyacetone (yield approximately 3%),[26,28,30,31] and formaldehyde.[30−34] In regions where low NO conditions lead to HO_x (sum of OH and HO_2) chemistry dominance, gas-phase isoprene oxidation leads to the formation of isoprene hydroxy hydroperoxides (ISOPOOH) (yield approximately 70%),[4,10,35] hydroperoxyenals (HPALDs) (yield approximately 5%),[36] methylbutenediol (yield smaller than 2%),[10] 3-methylfuran (yield up to 3%),[36−38] as well as methacrolein and methyl vinyl ketone (yield approximately 20−25% as sum of methacrolein and methyl vinyl ketone).[36−40] The major product under HO_x-dominated conditions is ISOPOOH with a yield of about 70%, which can be further oxidized by OH to yield isoprene epoxydiols (IEPOX) as major second generation oxidation product.[10] Recently, Bates et al. reported an estimated global annual production of IEPOX of 230 Tg y^{-1}.[41] Therefore, IEPOX represents a strong contributor to secondary organic aerosol (SOA) investigated in numerous studies of the recent past.[10,13,42−45] Effects associated with IEPOX SOA could influence climate forcing via the impact on the aerosol optical properties[46] as well as triggering health effects.[47] According to Bates et al., the loss of IEPOX from the gas phase under rural daytime conditions is attributed to particle uptake (approximately 19%), deposition (approximately 37%), and gas-phase oxidation (approximately 44%).[41] The particle uptake and subsequent reactions lead to C_5 alkenetriols,[44] IEPOX

Received: June 15, 2017
Revised: July 26, 2017
Published: July 28, 2017

DOI: 10.1021/acs.jpca.7b05879
J. Phys. Chem. A 2017, 121, 6460−6470

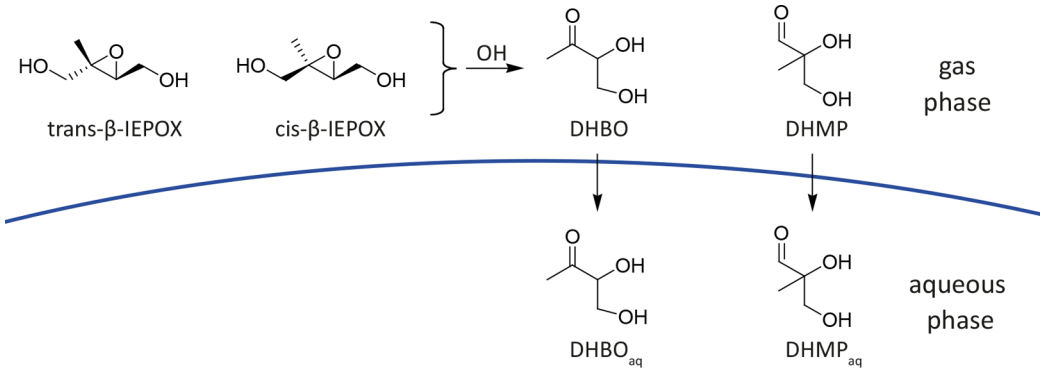

Figure 1. Depiction of the formation and the partitioning of the DHBO and DHMP.

organosulfates,[12,15,48−51] 3-methyltetrahydrofuran-3,4-diols,[13] 2-methanetetrols,[52] and dimeric species of IEPOX and IEPOX organosulfates.[12] The considered gas-phase oxidation leads to the formation of C_4 dihydroxycarbonyl compounds, C_4 hydroxydicarbonyl compounds, and smaller carbonyl compounds.[16,41,53] The studies by Bates et al. have shown that these C_4 dihydroxycarbonyl compounds, 3,4-dihydroxy-2-butanone (DHBO) and 2,3-dihydroxy-2-methylpropanal (DHMP), represent 46 ± 15% of the formed oxidation products.[41] Both DHBO and DHMP can be expected to be very water-soluble and hence undergo phase transfer to the tropospheric aqueous phase (Figure 1), as supposed by their estimated Henry's Law constants, $H^{cp}_{(DHBO)} \approx 2666$ mol L^{-1} atm^{-1} and $H^{cp}_{(DHMP)} \approx 1466$ mol L^{-1} atm^{-1}, derived by Estimation Programs Interface Suite/HenryWin.[54,55] The estimated vapor pressures of the compounds, $p^0_{(DHBO)}(298\ K) = 2.44 \times 10^{-5}$ atm and $p^0_{(DHMP)}(298\ K) = 1.60 \times 10^{-4}$ atm,[56] also indicate effective transfer from the gas phase to the aqueous phase. Therefore, further aqueous-phase oxidation and particularly the formation of product species may be expected to contribute to the formation of aqSOA, which is the main motivation for the present study.

Hence, aqueous-phase kinetics of the radical-driven oxidation of DHBO and DHMP with OH, NO_3, and SO_4^- as well as product studies for the subset of reactions of DHBO and DHMP with OH in aqueous solution have been performed to investigate in detail their impact on the formation of aqSOA. Aqueous-phase oxidation schemes based on the experimentally obtained results are suggested.

EXPERIMENTAL METHODS

Kinetics. Rate constants of the radical-driven oxidation reactions were obtained using a laser flash photolysis−laser long path absorption (LFP-LLPA) setup (Figure 2), similar to setups used in our former studies.[57,58] The thermostated measurement cell (278−318 K) made of nonfluorescing high-quality silica glass is continuously perfused by a solution containing the organic compound, the radical precursor and, in the case of OH kinetics, potassium thiocyanate as the reference compound.

For OH radical reaction kinetics, the radical precursor (H_2O_2, 2×10^{-4} mol L^{-1}) is photolyzed by an excimer laser (Compex 201, Coherent) flash at 248 nm. The formed OH radicals cannot be detected directly, due to their absorption band in the UV overlapping with the organic constituents. Therefore, the competition kinetics method was applied using potassium thiocyanate (2×10^{-5} mol L^{-1}) as reference.[59]

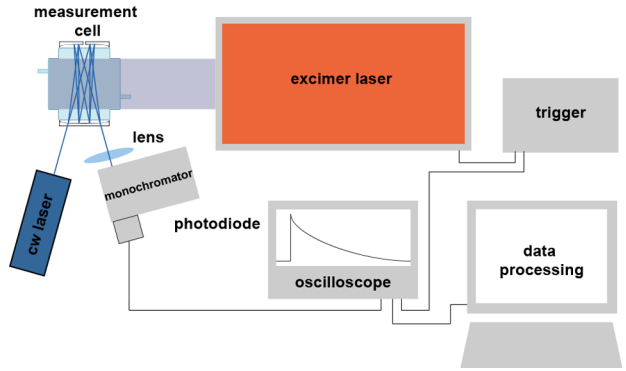

Figure 2. Scheme of the LFP-LLPA setup for kinetic investigations.

Thiocyanate anions react via the following reactions R-1−R-3) to dithiocyanate radical anions ($(SCN)_2^-$) detectable at 473 nm:

$$OH + SCN^- \rightleftharpoons SCNOH^- \quad \text{(R-1)}$$

$$SCNOH^- \rightleftharpoons SCN + OH^- \quad \text{(R-2)}$$

$$SCN + SCN^- \rightleftharpoons (SCN)_2^- \quad \text{(R-3)}$$

If the solution contains also an organic compound, there will be a competition between reaction R-1 above and reaction R-4:

$$OH + \text{organic compound} \rightleftharpoons \text{products} \quad \text{(R-4)}$$

The temperature-dependent reaction rate constant k_{ref} of the initial reaction R-1 has been determined by Chin and Wine[59] as

$$\ln k_{ref}(T) = (29.614 \pm 0.636) - (1900 \pm 190)/T \text{ L mol}^{-1} \text{ s}^{-1} \quad (1)$$

The reaction rate constant $k_{R\text{-}4}$ can be solved from eq 2[60]

$$\frac{A_{[(SCN)_2^-]_0}}{A_{[(SCN)_2^-]_X}} = \frac{k_{R\text{-}4}[\text{organic compound}]}{k_{ref}[SCN^-]} + 1 \quad (2)$$

A continuous-wave laser (cw-laser) (LasNOVA 40, Lasos) emitting at $\lambda = 473$ nm and a photodiode were used to detect the absorption of $(SCN)_2^-$, denoted by $A_{[(SCN)_2^-]_0}$ and $A_{[(SCN)_2^-]_x}$ where the subscripts x and 0 refer to organics being present or not. The laser beam passes through the measurement cell 12 times using a White mirror cell optic[61] to increase the optical path length to 84 cm and subsequently the sensitivity. The signals were recorded by an oscilloscope

DOI: 10.1021/acs.jpca.7b05879
J. Phys. Chem. A 2017, 121, 6460−6470

Table 1. Experimental Details of the Performed Product Studies

exp. no	description	irradiation	[compound]/mol L^{-1}	$[H_2O_2]$/mol L^{-1}	T/K	exp time/h	n^a
1	dark reaction H_2O_2 + DHBO		1×10^{-4}	5×10^{-3}	298	6	1
2	photolysis of DHBO	+	1×10^{-4}		298	6	1
3	OH-driven oxidation of DHBO	+	1×10^{-4}	5×10^{-3}	298	6	2
4	dark reaction H_2O_2 + DHMP		1×10^{-4}	5×10^{-3}	298	6	1
5	photolysis of DHMP	+	1×10^{-4}		298	6	1
6	OH-driven oxidation of DHMP	+	1×10^{-4}	5×10^{-3}	298	6	2

[a]Number of repetitions.

(Classic Delta, Gould Instrument System) and transferred to a computer for further data processing.

In the case of SO_4^- radical kinetics, the same experimental setup was used. Here, sodium persulfate ($Na_2S_2O_8$, 2.5×10^{-4} mol L^{-1}) was used as the radical precursor to be directly photolyzed to SO_4^- radicals. The obtained signal−time profiles were directly converted to absorbance−time profiles, which can then be kinetically evaluated. The linear regression of the natural logarithm of absorbance directly gave the first-order reaction rate constant k_{first}. The linear regression of the measured k_{first} dependent on [organic compound] then resulted in the second-order rate constant.[62]

In the case of NO_3 measurements a He−Ne laser (35-2, Spindler and Hoyer) emitting at 635 nm was used as analysis light source and the signal−time profiles were treated as described above.[63]

Mechanistic Investigation and Analytical Procedure. The product studies were performed in a 300 mL temperature-controlled aqueous-phase photoreactor. The reactor is equipped with a quartz glass window to irradiate the sample solution with an arc light source (LSH601, LOT Quantum Design) equipped with a xenon short arc lamp (450W, LSB541, LOT Quantum Design). To keep the temperature constant at 298 K, the photoreactor was thermostated. As the hydroxyl radical source, hydrogen peroxide was photolyzed in the OH-driven oxidation experiments and not in the hydrogen peroxide-driven dark experiments. Glass filters (5 mm WG 295 and 5 mm WG305) were applied to absorb light below 290 nm efficiently and mimic the actinic spectrum to avoid any possible complication by short wavelength photolysis of the educts or, possibly even more important, of transient products susceptible to short wavelength photolysis.

In general, the experiments were conducted using concentrations of 5×10^{-3} mol L^{-1} hydrogen peroxide and 1×10^{-4} mol L^{-1} of the organic compound. The initial pH was 6.0 ± 0.1 and unbuffered yielding lower pH during the experiment time. The experimental details summarized in Table 1 give an overview about performed experiments. During the experiment, samples were taken at intervals of 15 min for 3 h and afterward at intervals of 30 min.

RESULTS AND DISCUSSION

Kinetics. The target compounds DHBO and DHMP were investigated with regard to the kinetics of their oxidation reactions by OH, NO_3, and SO_4^- radicals. To the authors' knowledge, these aqueous-phase rate constants were not reported until present. The obtained temperature-dependent second-order rate constants are summarized in Table 2. Errors given in this table are statistical (n = 8) with 95% confidence interval considering Student's t-factor.

OH Kinetics. Investigations of the kinetics of similar organic compounds with OH radicals were already the focus of previous studies. Gligorovski et al. reported a second-order rate constant (k_{second}(298 K)) for hydroxyacetone + OH of (1.2 ± 0.1) × 10^9 L mol^{-1} s^{-1}.[64] Furthermore, Hesper determined for the reaction 2-hydroxy-3-butanone a second order rate constants of (2.9 ± 1.0) × 10^9 L mol^{-1} s^{-1}.[65] These compounds are similar to the compounds investigated in this study because they are all α-hydroxycarbonyls. Accordingly, the second-order rate constants are found to be in same range (cf. Table 2). Finally, the second-order reaction rate constants for DHBO and DHMP show a weak temperature dependence (cf. Figure 3). The obtained activation energies of E_A(DHBO) = 4.2 ± 2.7 kJ mol^{-1} and E_A(DHMP) = 3.2 ± 2.2 kJ mol^{-1} are remarkably small.

Table 2. Measured Second-Order Rate Constants for DHBO and DHMP with OH, NO_3, and SO_4^- Radicals at 298 K

	OH	NO_3	SO_4^-
compound	k_{second}/10^9 L mol^{-1} s^{-1}	k_{second}/10^6 L mol^{-1} s^{-1}	k_{second}/10^7 L mol^{-1} s^{-1}
DHBO	1.0 ± 0.1	2.6 ± 1.6	2.3 ± 0.2
DHMP	1.2 ± 0.1	7.9 ± 0.7	3.3 ± 0.2

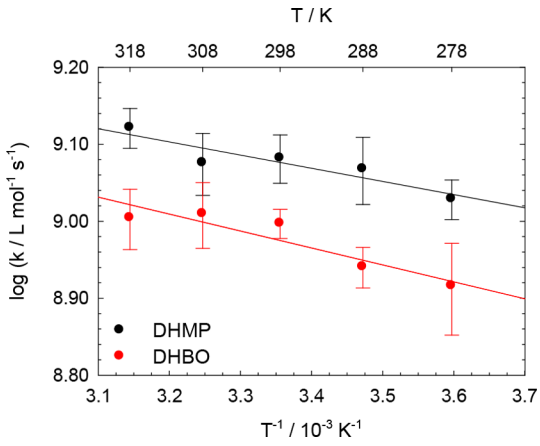

Figure 3. Arrhenius plot for the radical reactions of DHBO and DHMP with OH radicals.

Table 3. Applied Parameters for the Calculation of the Diffusion Constants

compound	V_m/cm^3 mol^{-1}	r/Å	D/cm^2 s^{-1}
DHBO	111.4[a]	3.53	9.35×10^{-6}
DHMP	113.8[a]	3.55	9.23×10^{-6}
OH	26.9[b]	2.20[b]	2.19×10^{-5}
NO_3	46.4[b]	2.64[b]	1.58×10^{-5}
SO_4^-	61.5[b]	2.90[b]	1.34×10^{-5}

[a]Estimated after the Joback method.[71] [b]Taken from Schöne et al.[66]

DOI: 10.1021/acs.jpca.7b05879
J. Phys. Chem. A 2017, 121, 6460−6470

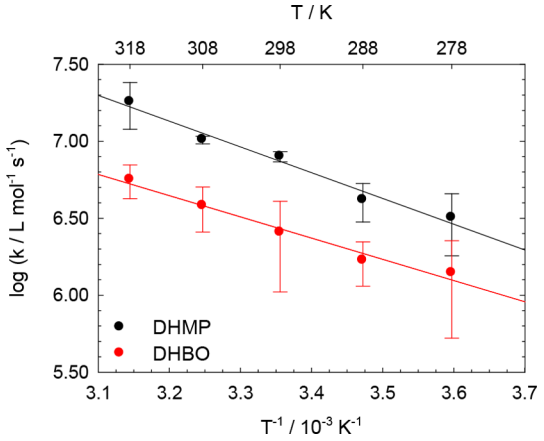

Figure 4. Arrhenius plot for the radical reactions of DHBO and DHMP with NO_3 radicals.

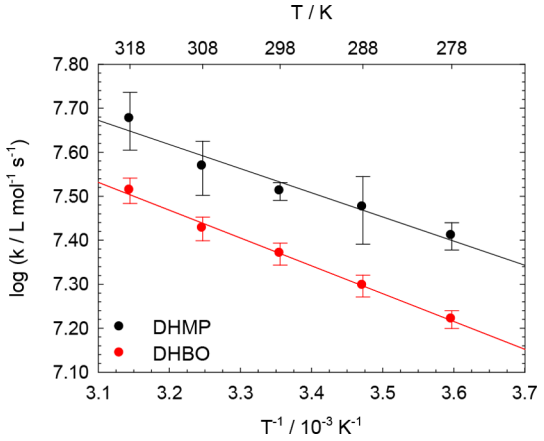

Figure 5. Arrhenius plot for the radical reactions of DHBO and DHMP with SO_4^- radicals.

Because the obtained second-order rate constants are near the diffusion limit, we calculated the diffusion constant k_D via the following procedure described in Schöne et al.[66] The Smoluchowski equation (3) defines the diffusion constant k_D:[67]

$$k_D = 4 \times 10^3 \times \pi \times N_A \times (D_{rad} + D_{or}) \times (r_{rad} + r_{or}) \quad (3)$$

Here D_{rad} and D_{or} represent the diffusion coefficients of the radical and the organic compound, whereas r_{rad} and r_{or} stand for the radii of the radical and organic compound and N_A is the Avogadro constant. The required diffusion coefficients are calculated via a modified Stokes−Einstein relationship:[68]

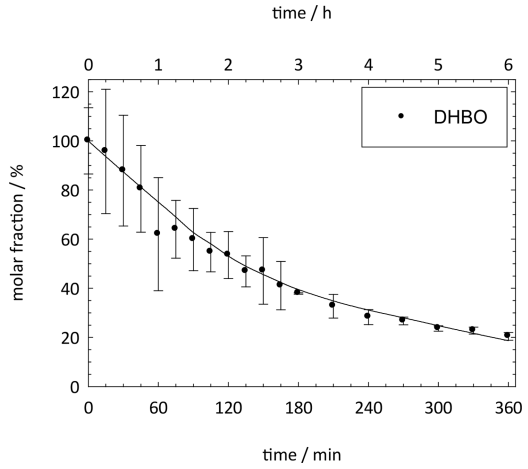

Figure 6. Averaged molar fraction of DHBO (n = 2) during the oxidation experiments as a function of time.

$$D = 7.4 \times 10^{-8} \times \frac{(XM)^{0.5} \times T}{V_m^{0.6} \times \eta} \quad (4)$$

where V_m represents the molar volume at 298 K, T is the temperature (298 K), η is the viscosity of water (η = 0.89 g cm^{-1} s^{-1}[69]), X is the association parameter of water (2.26), and M is the molar mass of water. The radii of the molecules are calculated following eq 5:[70]

$$r = \sqrt[3]{\frac{3V_m}{4\pi N_A}} \quad (5)$$

Table 3 summarizes all applied parameters for the method described above.

Estimated diffusion rate constants for both compounds are $k_D \approx 1.36 \times 10^{10}$ L mol^{-1} s^{-1}. Therefore, the contribution to the obtained second order rate constants k_{second} of the reactions with OH radicals is 7.3% for DHBO and 8.9% for DHMP and the reaction rate constants are still dominated by the chemical activation.

NO_3 Kinetics. Compared to reaction rate constants of NO_3 with carbonyls (k_{second} = 6.9 × 10^6 to 5.8 × 10^7 L mol^{-1} s^{-1}) reported in the literature,[62,66] the reaction rate constants obtained here are in the same range. Interestingly, the nitrate radical reactions show the strongest temperature dependence, compared to the OH and SO_4^- reactions (cf. Figure 4 and Table 3); thus the highest activation energies are 26.4 kJ mol^{-1} for DHBO + NO_3 and 32.0 kJ mol^{-1} for DHMP + NO_3.

The diffusion rate constants at 298 K for the reactions of NO_3 with DHBO and DHMP are approximately 1.17 × 10^{10} L mol^{-1} s^{-1}, 4 orders of magnitude higher than the determined

Table 4. Obtained Arrhenius Parameters of the Reactions of DHBO and DHMP with OH, NO_3 and SO_4^- radicals

compound	radical	A/s^{-1} [a]	E_A/kJ mol^{-1} [b]	$\Delta G^{\ddagger}$/kJ mol^{-1} [c]	$\Delta H^{\ddagger}$/kJ mol^{-1} [d]	$\Delta S^{\ddagger}$/J mol^{-1} K^{-1} [e]
DHBO	OH	(5.2 ± 0.3) × 10^9	4.2 ± 2.7	21.8 ± 15.2	1.7 ± 1.1	−67.3 ± 3.3
	NO_3	(1.1 ± 0.1) × 10^{11}	26.4 ± 6.3	36.3 ± 12.9	23.9 ± 5.7	−41.6 ± 4.8
	SO_4^-	(3.1 ± 0.1) × 10^9	12.1 ± 1.4	30.9 ± 4.3	9.6 ± 1.1	−71.5 ± 1.8
DHMP	OH	(4.4 ± 0.2) × 10^9	3.2 ± 2.2	21.2 ± 15.2	0.7 ± 0.5	−68.7 ± 2.7
	NO_3	(3.0 ± 0.4) × 10^{12}	32.0 ± 7.9	33.8 ± 12.1	29.5 ± 7.3	−14.3 ± 1.6
	SO_4^-	(2.4 ± 0.2) × 10^9	10.5 ± 3.8	30.0 ± 12.9	8.0 ± 2.9	−73.8 ± 5.2

[a]Pre-exponential factor. [b]activation energy. [c]Gibbs' free energy of activation. [d]Enthalpy of activation. [e]Entropy of activation.

DOI: 10.1021/acs.jpca.7b05879
J. Phys. Chem. A 2017, 121, 6460−6470

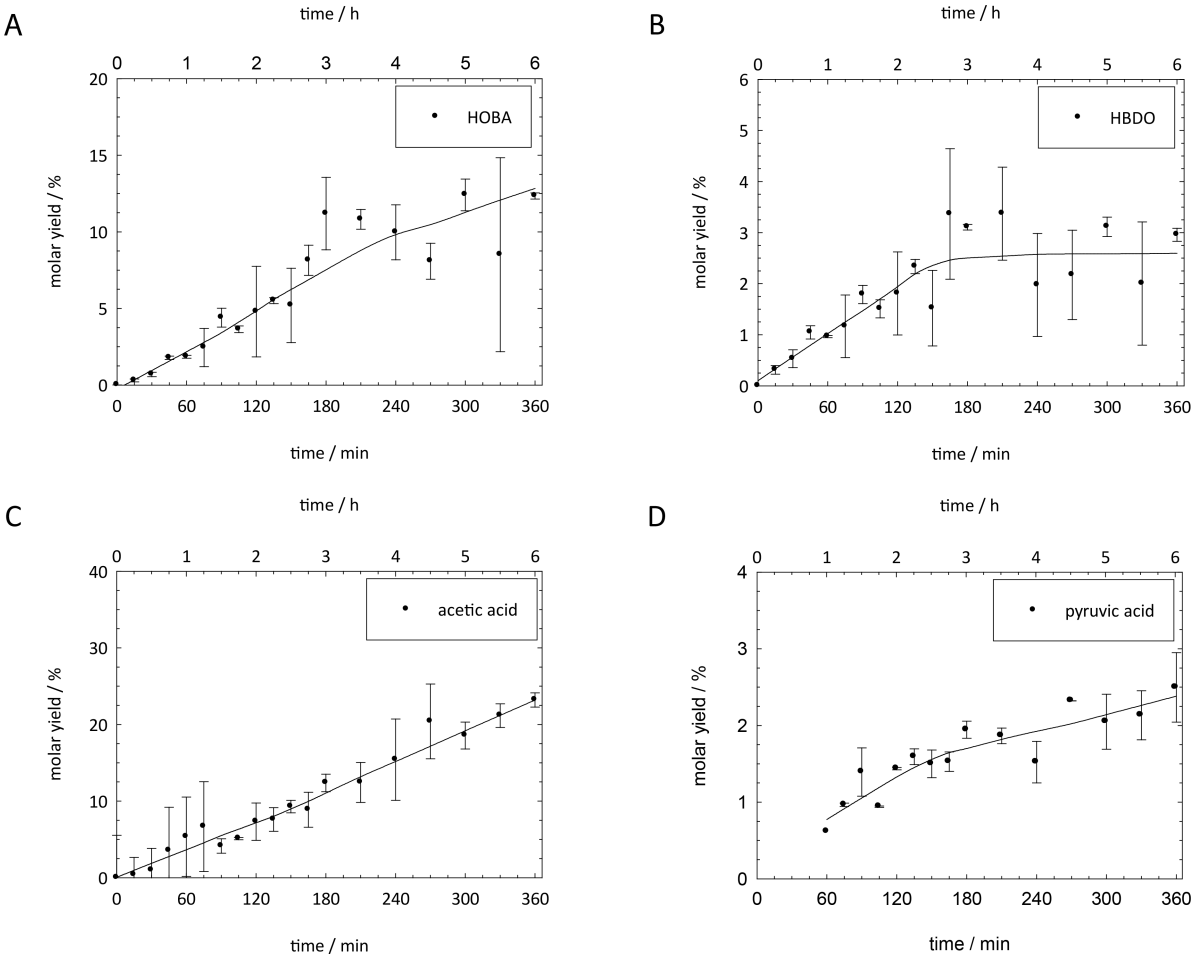

Figure 7. Averaged molar yields of HOBA (A), HBDO (B), acetic acid (C), and pyruvic acid (D) (n = 2) during the oxidation experiments of DHBO as a function of time.

rate constants, and accordingly, the rate constants are fully chemically controlled.

SO_4^- Kinetics. The SO_4^- kinetics complete the set of investigated reactions. Both reactions studied show a weak temperature dependence, as can be seen from Figure 5. These temperature dependences result in activation energies around 10 kJ mol^{-1} (cf. Table 4).

The diffusion rate constants at 298 K for the reactions of SO_4^- with DHBO and DHMP are about 1.10 × 10^{10} L mol^{-1} s^{-1}, yielding to a contribution less than 0.5% to the determined rate constants so that chemical control governs these reaction.

Activation Parameters. In general, obtained activation parameters are similar for reactions with both compounds. When the three radicals are compared with each other, there is a trend in the activation energies: E_A(OH) is smaller than $E_A(SO_4^-)$ than $E_A(NO_3)$. The pre-exponential factors of the NO_3 reactions are 2 and 3 orders of magnitude higher compared to those for OH and SO_4^-, respectively, corresponding to weak entropy changes in the course of the latter reactions. Table 4 shows all calculated activation parameters of the investigated radical reactions of DHBO and DHMP. Errors given in this table are statistical (n = 5) with 95% confidence interval considering Student's t-factor.

DHBO + OH Oxidation Products. In Figure 6 the molar fraction of DHBO as a function of time is shown. During the experiment time of 6 h ~80% of the initial DHBO is degraded to its oxidation products. The error bars in all following time profiles are the 1σ standard deviation (n = 2) and the solid line represents a smoothed trend (LOWESS (locally weighted scatterplot smoothing), smoothing parameter f = 0.7, 3 iterations).

Runs of a model using Copasi 4.19 (see the Supporting Information) lead to an OH concentration for these oxidation experiments of [OH] ≈ 1 × 10^{-13} mol L^{-1} (cf. Figure S1), which should possibly be regarded as an upper limit due to still missing sink reactions, such as the reaction of formed oxidation products with OH. The resulting OH concentration is in good agreement with a recent study on the oxidation of oxy aromatics at the air−water interface[72] and modeled bulk concentrations.[60]

The most favored reaction sites with respect to an OH-initiated oxidation of DHBO are the hydroxy group substituted C3 and C4 positions, which will lead to the formation of 1-hydroxy-2,3-butadione (HBDO) and 2-hydroxy-3-oxobutanal (HOBA). Both of these main pathways reveal a ratio of 1:4. These findings are consistent with the 1:4 ratio of the rate constants estimated with the structure−activity relationship by Monod and Doussin for these pathways, k_{C4} = 6.0 × 10^8 L mol^{-1} s^{-1} and k_{C3} = 1.4 × 10^8 L mol^{-1} s^{-1}.[72,73] The molar yield of HOBA obtained for the oxidation experiments is depicted in Figure 7A as a function of time.

As can be seen from Figure 7A, HOBA is formed with a maximum yield of ≈12%. Contrasting to this, HBDO is only formed with a yield of ≈3% (cf. Figure 7B).

DOI: 10.1021/acs.jpca.7b05879
J. Phys. Chem. A 2017, 121, 6460−6470

Scheme 1. Proposed Oxidation Mechanism of DHBO in the Aqueous Phase (Observed Products in Red Boxes)

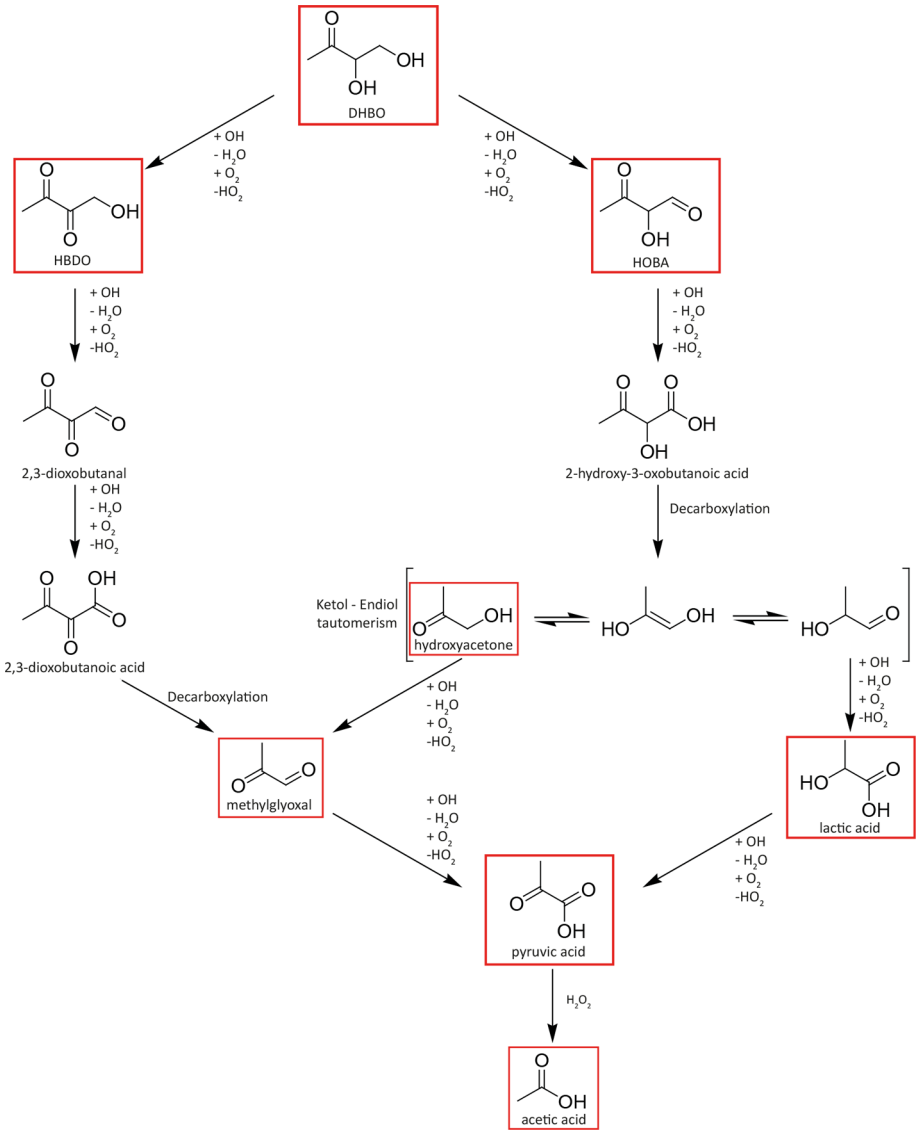

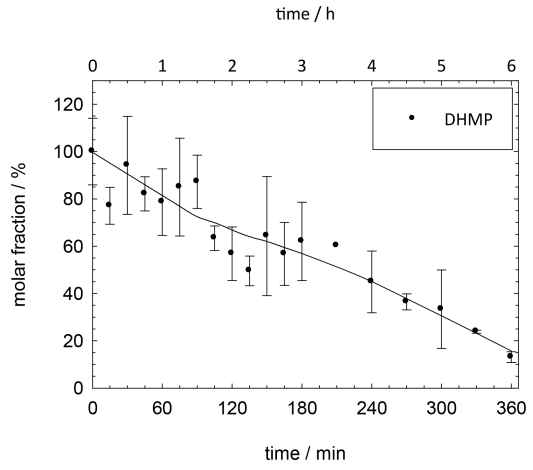

Figure 8. Averaged molar fraction of DHMP (n = 2) during the oxidation experiments as a function of time.

In line with the prediction from thermochemistry, these two pathways (Scheme 1) are the most important ones following H-abstraction. Another main product within these experiments is acetic acid, which is constantly formed with a maximum yield of 23% at 6 h (cf. Figure 7C).

The surprisingly high yield of acetic acid can be formed via the intermediate pyruvic acid (cf. Figure 7D), which is further reacting with H_2O_2 via the mechanism in the literature.[74,75] The direct photolysis of pyruvic acid studied by Eugene and Guzman showed a remarkable low concentration of acetic acid,[76] which leads to the finding that the degradation of the formed pyruvic acid in the present study is dominated by the H_2O_2-driven mechanism under the applied conditions.

Apparently, the degradation of pyruvic acid in our system is caused neither by OH oxidation nor by direct photolysis but is linked to it due to the applied H_2O_2 concentration ($[H_2O_2] = 5 \times 10^{-3}$ mol L^{-1}), cf. Figure S9. A major fraction of acetic acid measured results from converted pyruvic acid. Compared to expected hydrogen peroxide concentration levels of 4×10^{-4} and 6×10^{-5} mol L^{-1} for aerosol liquid water (ALW) and cloudwater under remote daytime conditions, respectively, this applied concentration of hydrogen peroxide is certainly higher than the calculated values. Therefore, the direct photolysis of pyruvic acid could become more relevant and the formation of

DOI: 10.1021/acs.jpca.7b05879
J. Phys. Chem. A 2017, 121, 6460−6470

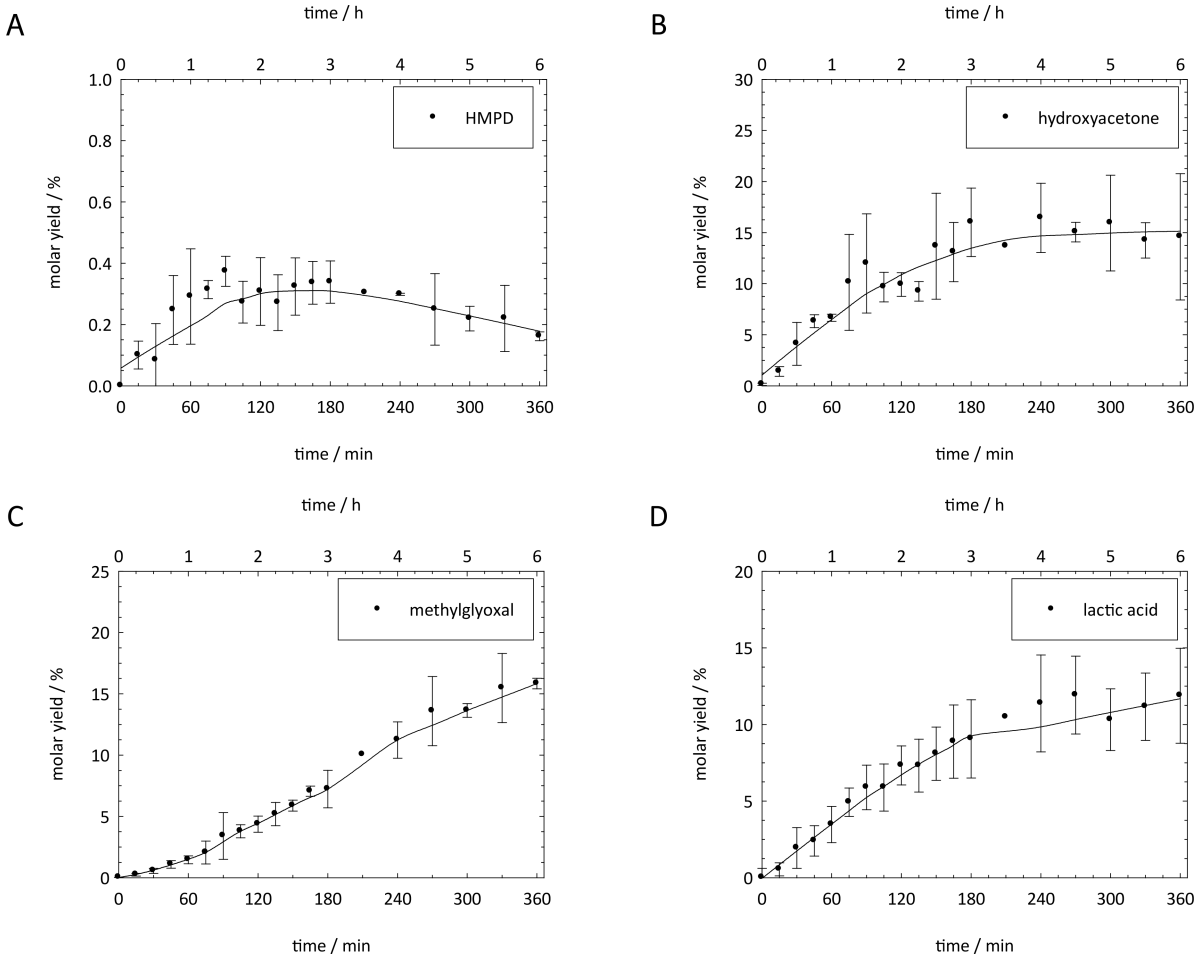

Figure 9. Averaged molar yield of HMPD (A), hydroxyacetone (B), methylglyoxal (C), and lactic acid (D) (n = 2) during the oxidation experiments of DHMP as a function of time.

acetic acid via the proposed pathway might be less effective if the hydrogen peroxide concentration is in an atmospherically relevant range.

Additionally, hydroxyacetone, methylglyoxal and lactic acid were determined as intermediates. Although their yields are smaller than 3% (cf. Figure S2–S4). These species are intermediates in the reaction pathways down to acetic acid.

Besides the oxidation, there is still the direct photolysis of DHBO leading to glycolaldehyde, glyoxal, oxalic acid, and glyoxalic acid, which can also act as precursor for aqSOA formation.[77] But this pathway is negligible due to the absorption branching ratio of H_2O_2 ($\varepsilon_{300\ nm}$ = 0.55 L mol^{-1} cm^{-1}) versus DHBO ($\varepsilon_{300\ nm}$ = 3.72 L mol^{-1} cm^{-1}) of approximately 120:1.

Overall, the oxidation mechanism of DHBO can be postulated as shown in Scheme 1. DHBO is predominantly present as unhydrated ketone (96.9%) following estimated by the structure–activity relationship of Raventos-Duran et al.[78] Therefore, its first generation oxidation products in the aqueous-phase HBDO and HOBA are formed via H-abstraction followed by oxygen addition and HO_2 elimination as final step. The following hypothesized stable reaction products, 2,3-dioxobutanal, 2,3-dioxobutanoic acid, and 2-hydroxy-3-oxobutanoic acid cannot be observed via the techniques applied in the present study. Next in the mechanism, 2-hydroxy-3-oxobutanoic acid decarboxylates after a cyclic rearrangement mechanism. The formed enol undergoes a ketol–enediol tautomerism similar to the Lobry de Bruyn–van Ekenstein transformation[79] to explain the observed hydroxyacetone. The further product lactaldehyde is not observed; however, the subsequent oxidation product lactic acid is detected. Lactic acid is again oxidized via H-abstraction followed by oxygen addition and HO_2 elimination to yield pyruvic acid. Hydroxyacetone being formed can be further oxidized following a similar mechanism yielding methylglyoxal as outlined by Schaefer et al.,[80] which is then also oxidized to pyruvic acid. The formed pyruvic acid is a potential precursor for the formation of oligomers under UV irradiation as outlined in a recent study.[76] However, these types of products were not in the focus of the present investigation.

Another possible source of methylglyoxal is the oxidation of 2,3-dioxobutanal to 2,3-dioxobutanoic acid followed by a decarboxylation. After 6 h approximately 75% of the produced organic mass is explained by this mechanism (cf. Figure S5).

DHMP + OH Oxidation Products. The oxidation experiments of DHMP are also conducted over 6 h. DHMP is oxidized down to a molar fraction of 13% during the experiment as depicted in Figure 8.

The most probable reaction sides for an H-abstraction by OH radicals are the H atoms at the carbonyl carbon and the CH_2 group estimated by the structure–activity relationship by Monod and Doussin.[72,73] Accordingly, the oxidation will lead to 2-hydroxy-2-methylpropanedial (HMPD), also known as methylreductone, which is thought to be very instable.[81]

DOI: 10.1021/acs.jpca.7b05879
J. Phys. Chem. A 2017, 121, 6460–6470

Scheme 2. Proposed Oxidation Mechanism of DHMP in the Aqueous Phase (Observed Products in Red Boxes)

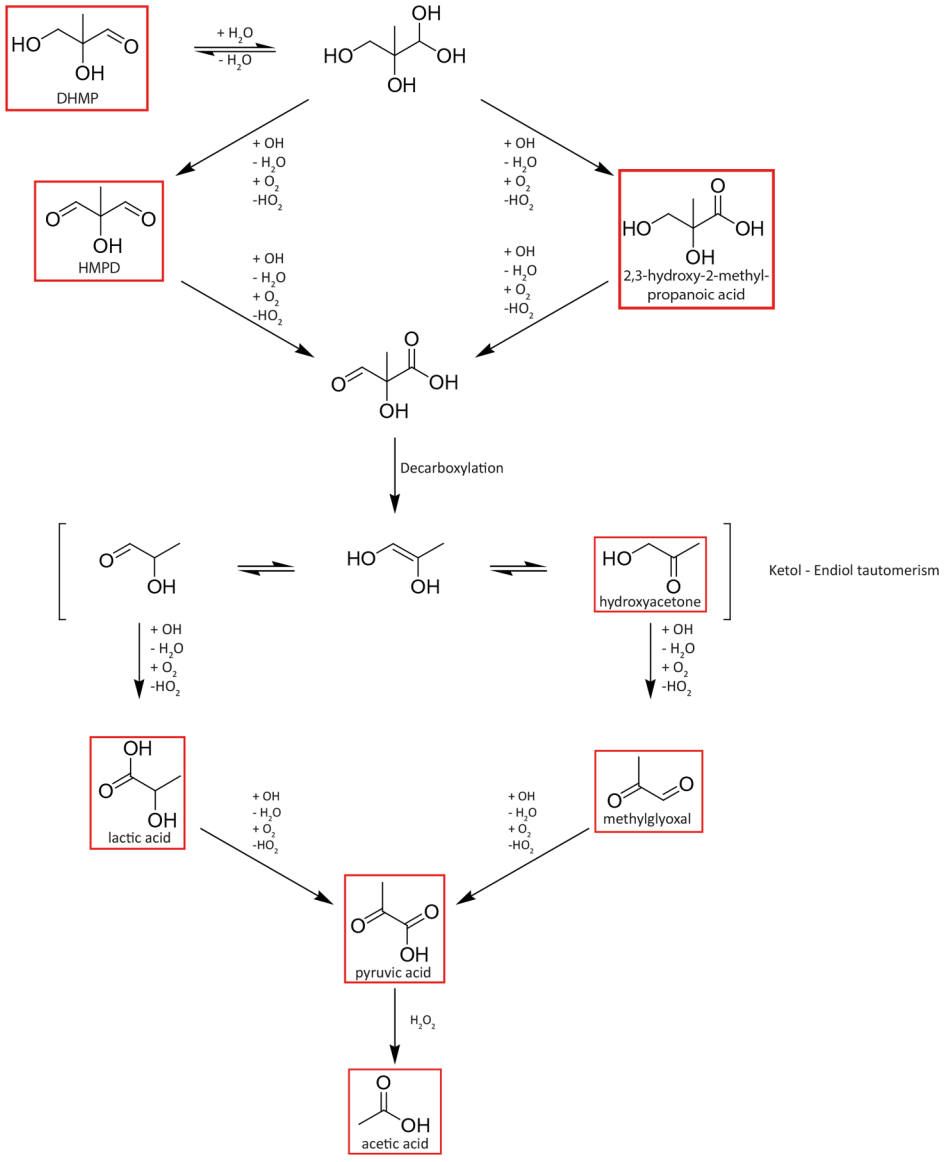

Therefore, it is only observed in minor yields as it is shown in Figure 9A.

The second estimated first generation oxidation product is 2,3-hydroxy-2-methylpropanoic acid tentatively identified by UPLC-HDMS measurements. Here we observed a product fraction at a retention time of 0.73 min with a mass spectrum (cf. Figure S6) showing a mass to charge ratio of 119.0349, which is assigned to the $[M - H^+]$ molecule of 2,3-hydroxy-2-methylpropanoic acid (calculated m/z = 119.0344).

The major products of OH-initiated oxidation were hydroxyacetone, methylglyoxal, lactic acid, and pyruvic acid. Hydroxyacetone is formed up to a yield of 16.5% after 4 h and stays constant due to equal rates of formation and further oxidation as shown in Figure 9B.

The shape of the shown molar yield time profile leads to the assumption that hydroxyacetone is a first or second generation oxidation product of DHMP. Consecutively, methylglyoxal is formed as discussed in the section DHBO + OH Oxidation Products as an oxidation product of hydroxyacetone. The yield−time profile (cf. Figure 9C) supports this hypothesis by the shown behavior like a subsequent product with a significantly increasing yield after approximately 1.5 h while hydroxyacetone is significantly formed after 0.5 h.

Pyruvic acid is only represented by up to 3.3% (cf. Figure S7) due to its intermediate nature and the fast oxidation caused by the applied concentration of hydrogen peroxide as discussed before.

In contrast, lactic acid is a major product with a yield up to 12% in the OH-initiated aqueous-phase oxidation of DHMP compared to the oxidation of DHBO where it is only formed with yields up to 3%. As shown in Figure 9D, the yield of lactic acid seems to stagnate after 3.5 h. This finding leads to the assumption that the fluxes of the source and sink reactions are equal in the range of 3.5 h up to 6 h.

In conclusion, the proposed OH-initiated oxidation mechanism of DHMP is depicted in Scheme 2. First generation oxidation products of the hydrated and unhydrated DHMP (the hydration equilibrium constant K_{hyd} of DHMP is estimated to be 9.77 after the structure−activity relationship by Raventos-Duran et al.[78]) are 2-hydroxy-2-methylpropanedial (HMPD) and 2,3-dihydroxy-2-methylpropanoic acid formed via H-abstraction followed by oxygen addition and HO_2 elimination.

DOI: 10.1021/acs.jpca.7b05879
J. Phys. Chem. A 2017, 121, 6460−6470

The following multifunctional intermediate product 2-hydroxy-3-oxopropanoic acid is supposed to be formed via the same mechanism from both first generation oxidation products but is not observed in this study. Then, a subsequent decarboxylation leads to the observed hydroxyacetone and lactaldehyde. Finally, the oxidation of these products follows the same mechanism as described in the previous section leading to pyruvic acid and, for the applied experimental conditions, to acetic acid. The reaction pathway of pyruvic acid with hydrogen peroxide will be less important under atmospherically relevant conditions and the OH-driven oxidation and direct photochemistry of pyruvic acid might become more relevant depending on atmospheric aqueous-phase H_2O_2 concentrations. Overall, 67% of the molar conversion of this experiment is explainable after 6 h (cf. Figure S8).

CONCLUSION

The present study describes the aqueous-phase reactivity of the isoprene-derived dihydroxycarbonyl compounds DHBO and DHMP toward atmospherically relevant oxidants OH, NO_3, and SO_4^- radicals. Due to the atmospheric abundance of OH radicals and the second-order rate constants of the reactions with OH, the OH-initiated oxidation of these isoprene-derived dihydroxycarbonyls is the main radical-driven degradation pathway in the tropospheric aqueous phase. The investigation of the kinetics reveals that at least the OH reaction rate constants are fast but reach only fractional diffusion control. As an extension of the present study, the nonradical-driven aqueous-phase oxidation of these constituents are not clear at present and should be investigated.

The performed OH-driven aqueous-phase product studies show the formation of hydroxydicarbonyls (such as HBDO, HOBA, and HMPD), smaller carbonyls and dicarbonyls (such as methylglyoxal and hydroxyacetone), and smaller carboxylic acids (such as lactic and pyruvic acid). It is interesting to note that pyruvic acid is efficiently converted to acetic acid when hydrogen peroxide is present in the aqueous phase. Methylglyoxal and hydroxyacetone, which are also formed in the present study, are discussed as SOA and aqSOA precursors. Therefore, the investigated dihydroxycarbonyls are potential aqSOA precursors.

Overall, the obtained kinetic results and the observed major mechanistic pathways leading to the suggested reaction schemes represent a good basis to describe the aqueous-phase fate of isoprene-derived compounds more precisely. The presented findings will be implemented in the Chemical Aqueous-Phase Radical Mechanism (CAPRAM) to achieve a more detailed understanding on the atmospheric budget of compounds of interest.

ASSOCIATED CONTENT

Supporting Information

The Supporting Information is available free of charge on the ACS Publications website at DOI: 10.1021/acs.jpca.7b05879.

Sample preparation procedures, temperature-dependent second-order rate constants, yield time profiles, concentrations and reactions, turnover plots of the products studies, mass spectrum (PDF)

AUTHOR INFORMATION

Corresponding Author

*H. Herrmann. Phone: +49 341 2717 7024. Fax: +49 341 2717 99 7024. e-mail: herrmann@tropos.de.

ORCID

Hartmut Herrmann: 0000-0001-7044-2101

Notes

The authors declare no competing financial interest.

ACKNOWLEDGMENTS

This work was partly done in the framework of the MISOX II project (grant number HE 3086/13-3) funded by the DFG (German Research Foundation). Additionally, the authors are grateful for support by the European Regional Development Funds (EFRE - Europe funds Saxony) and the European Union for supporting the MARSU project (grant 690958) in HORIZON 2020.

REFERENCES

(1) Guenther, A. B.; Jiang, X.; Heald, C. L.; Sakulyanontvittaya, T.; Duhl, T.; Emmons, L. K.; Wang, X. The Model of Emissions of Gases and Aerosols from Nature version 2.1 (MEGAN2.1): an Extended and Updated Framework for Modeling Biogenic Emissions. *Geosci. Model Dev.* **2012**, *5*, 1471−1492.

(2) Sindelarova, K.; Granier, C.; Bouarar, I.; Guenther, A.; Tilmes, S.; Stavrakou, T.; Müller, J. F.; Kuhn, U.; Stefani, P.; Knorr, W. Global Data Set of Biogenic VOC Emissions Calculated by the MEGAN Model over the last 30 Years. *Atmos. Chem. Phys.* **2014**, *14*, 9317−9341.

(3) Dillon, T. J.; Crowley, J. N. Direct Detection of OH Formation in the Reactions of HO_2 with $CH_3C(O)O_2$ and other Substituted Peroxy Radicals. *Atmos. Chem. Phys.* **2008**, *8*, 4877−4889.

(4) Lelieveld, J.; Butler, T. M.; Crowley, J. N.; Dillon, T. J.; Fischer, H.; Ganzeveld, L.; Harder, H.; Lawrence, M. G.; Martinez, M.; Taraborrelli, D.; et al. Atmospheric Oxidation Capacity Sustained by a Tropical Forest. *Nature* **2008**, *452*, 737−740.

(5) Archibald, A. T.; Cooke, M. C.; Utembe, S. R.; Shallcross, D. E.; Derwent, R. G.; Jenkin, M. E. Impacts of Mechanistic Changes on HO_x Formation and Recycling in the Oxidation of Isoprene. *Atmos. Chem. Phys.* **2010**, *10*, 8097−8118.

(6) Claeys, M.; Graham, B.; Vas, G.; Wang, W.; Vermeylen, R.; Pashynska, V.; Cafmeyer, J.; Guyon, P.; Andreae, M. O.; Artaxo, P.; et al. Formation of Secondary Organic Aerosols Through Photooxidation of Isoprene. *Science* **2004**, *303*, 1173−1176.

(7) Surratt, J. D.; Murphy, S. M.; Kroll, J. H.; Ng, N. L.; Hildebrandt, L.; Sorooshian, A.; Szmigielski, R.; Vermeylen, R.; Maenhaut, W.; Claeys, M.; et al. Chemical Composition of Secondary Organic Aerosol Formed from the Photooxidation of Isoprene. *J. Phys. Chem. A* **2006**, *110*, 9665−9690.

(8) Kroll, J. H.; Ng, N. L.; Murphy, S. M.; Flagan, R. C.; Seinfeld, J. H. Secondary Organic Aerosol Formation from Isoprene Photooxidation. *Environ. Sci. Technol.* **2006**, *40*, 1869−1877.

(9) Kleindienst, T. E.; Edney, E. O.; Lewandowski, M.; Offenberg, J. H.; Jaoui, M. Secondary Organic Carbon and Aerosol Yields from the Irradiations of Isoprene and α-Pinene in the Presence of NO_x and SO_2. *Environ. Sci. Technol.* **2006**, *40*, 3807−3812.

(10) Paulot, F.; Crounse, J. D.; Kjaergaard, H. G.; Kürten, A.; St. Clair, J. M.; Seinfeld, J. H.; Wennberg, P. O. Unexpected Epoxide Formation in the Gas-Phase Photooxidation of Isoprene. *Science* **2009**, *325*, 730−733.

(11) Hallquist, M.; Wenger, J. C.; Baltensperger, U.; Rudich, Y.; Simpson, D.; Claeys, M.; Dommen, J.; Donahue, N. M.; George, C.; Goldstein, A. H.; et al. The Formation, Properties and Impact of Secondary Organic Aerosol: Current and Emerging Issues. *Atmos. Chem. Phys.* **2009**, *9*, 5155−5236.

DOI: 10.1021/acs.jpca.7b05879
J. Phys. Chem. A 2017, 121, 6460−6470

(12) Surratt, J. D.; Chan, A. W. H.; Eddingsaas, N. C.; Chan, M. N.; Loza, C. L.; Kwan, A. J.; Hersey, S. P.; Flagan, R. C.; Wennberg, P. O.; Seinfeld, J. H. Reactive Intermediates Revealed in Secondary Organic Aerosol Formation from Isoprene. *Proc. Natl. Acad. Sci. U. S. A.* **2010**, *107*, 6640−6645.
(13) Lin, Y. H.; Zhang, Z. F.; Docherty, K. S.; Zhang, H. F.; Budisulistiorini, S. H.; Rubitschun, C. L.; Shaw, S. L.; Knipping, E. M.; Edgerton, E. S.; Kleindienst, T. E.; et al. Isoprene Epoxydiols as Precursors to Secondary Organic Aerosol Formation: Acid-Catalyzed Reactive Uptake Studies with Authentic Compounds. *Environ. Sci. Technol.* **2012**, *46*, 250−258.
(14) Worton, D. R.; Surratt, J. D.; LaFranchi, B. W.; Chan, A. W. H.; Zhao, Y. L.; Weber, R. J.; Park, J. H.; Gilman, J. B.; de Gouw, J.; Park, C.; et al. Observational Insights into Aerosol Formation from Isoprene. *Environ. Sci. Technol.* **2013**, *47*, 11403−11413.
(15) Schindelka, J.; Iinuma, Y.; Hoffmann, D.; Herrmann, H. Sulfate Radical-Initiated Formation of Isoprene-Derived Organosulfates in Atmospheric Aerosols. *Faraday Discuss.* **2013**, *165*, 237−259.
(16) Bates, K. H.; Crounse, J. D.; Clair, J. M., St; Bennett, N. B.; Nguyen, T. B.; Seinfeld, J. H.; Stoltz, B. M.; Wennberg, P. O. Gas Phase Production and Loss of Isoprene Epoxydiols. *J. Phys. Chem. A* **2014**, *118*, 1237−1246.
(17) Nguyen, T. B.; Coggon, M. M.; Bates, K. H.; Zhang, X.; Schwantes, R. H.; Schilling, K. A.; Loza, C. L.; Flagan, R. C.; Wennberg, P. O.; Seinfeld, J. H. Organic Aerosol Formation from the Reactive Uptake of Isoprene Epoxydiols (IEPOX) onto Non-Acidified Inorganic Seeds. *Atmos. Chem. Phys.* **2014**, *14*, 3497−3510.
(18) Gaston, C. J.; Riedel, T. P.; Zhang, Z. F.; Gold, A.; Surratt, J. D.; Thornton, J. A. Reactive Uptake of an Isoprene-Derived Epoxydiol to Submicron Aerosol Particles. *Environ. Sci. Technol.* **2014**, *48*, 11178−11186.
(19) Liu, Y.; Kuwata, M.; Strick, B. F.; Geiger, F. M.; Thomson, R. J.; McKinney, K. A.; Martin, S. T. Uptake of Epoxydiol Isomers Accounts for Half of the Particle-Phase Material Produced from Isoprene Photooxidation via the HO_2 Pathway. *Environ. Sci. Technol.* **2015**, *49*, 250−258.
(20) Nguyen, T. B.; Bates, K. H.; Crounse, J. D.; Schwantes, R. H.; Zhang, X.; Kjaergaard, H. G.; Surratt, J. D.; Lin, P.; Laskin, A.; Seinfeld, J. H.; et al. Mechanism of the Hydroxyl Radical Oxidation of Methacryloyl Peroxynitrate (MPAN) and its Pathway toward Secondary Organic Aerosol Formation in the Atmosphere. *Phys. Chem. Chem. Phys.* **2015**, *17*, 17914−17926.
(21) Szmigielski, R. Evidence for C-5 Organosulfur Secondary Organic Aerosol Components from In-Cloud Processing of Isoprene: Role of Reactive SO_4 and SO_3 Radicals. *Atmos. Environ.* **2016**, *130*, 14−22.
(22) Xu, L.; Middlebrook, A. M.; Liao, J.; de Gouw, J. A.; Guo, H. Y.; Weber, R. J.; Nenes, A.; Lopez-Hilfiker, F. D.; Lee, B. H.; Thornton, J. A.; et al. Enhanced Formation of Isoprene-Derived Organic Aerosol in Sulfur-Rich Power Plant Plumes during Southeast Nexus. *J. Geophys. Res.: Atmos.* **2016**, *121*, 11137−11153.
(23) Riva, M.; Budisulistiorini, S. H.; Zhang, Z. F.; Gold, A.; Surratt, J. D. Chemical Characterization of Secondary Organic Aerosol Constituents from Isoprene Ozonolysis in the Presence of Acidic Aerosol. *Atmos. Environ.* **2016**, *130*, 5−13.
(24) Sprengnether, M.; Demerjian, K. L.; Donahue, N. M.; Anderson, J. G. Product Analysis of the OH Oxidation of Isoprene and 1,3-Butadiene in the Presence of NO. *J. Geophys. Res.* **2002**, *107*, ACH 8−1−ACH 8−13.
(25) Lockwood, A. L.; Shepson, P. B.; Fiddler, M. N.; Alaghmand, M. Isoprene Nitrates: Preparation, Separation, Identification, Yields, and Atmospheric Chemistry. *Atmos. Chem. Phys.* **2010**, *10*, 6169−6178.
(26) Paulot, F.; Crounse, J. D.; Kjaergaard, H. G.; Kroll, J. H.; Seinfeld, J. H.; Wennberg, P. O. Isoprene Photooxidation: New Insights into the Production of Acids and Organic Nitrates. *Atmos. Chem. Phys.* **2009**, *9*, 1479−1501.
(27) Baker, J.; Arey, J.; Atkinson, R. Formation and Reaction of Hydroxycarbonyls from the Reaction of OH Radicals with 1,3-Butadiene and Isoprene. *Environ. Sci. Technol.* **2005**, *39*, 4091−4099.
(28) Zhao, J.; Zhang, R.; Fortner, E. C.; North, S. W. Quantification of Hydroxycarbonyls from OH−Isoprene Reactions. *J. Am. Chem. Soc.* **2004**, *126*, 2686−2687.
(29) Dibble, T. S. Isomerization of OH-Isoprene Adducts and Hydroxyalkoxy Isoprene Radicals. *J. Phys. Chem. A* **2002**, *106*, 6643−6650.
(30) Galloway, M. M.; Huisman, A. J.; Yee, L. D.; Chan, A. W. H.; Loza, C. L.; Seinfeld, J. H.; Keutsch, F. N. Yields of Oxidized Volatile Organic Compounds during the OH Radical Initiated Oxidation of Isoprene, Methyl Vinyl Ketone, and Methacrolein under High-NO_x Conditions. *Atmos. Chem. Phys.* **2011**, *11*, 10779−10790.
(31) Dibble, T. S. Prompt Chemistry of Alkenoxy Radical Products of the Double H-Atom Transfer of Alkoxy Radicals from Isoprene. *J. Phys. Chem. A* **2004**, *108*, 2208−2215.
(32) Bregonzio-Rozier, L.; Siekmann, F.; Giorio, C.; Pangui, E.; Morales, S. B.; Temime-Roussel, B.; Gratien, A.; Michoud, V.; Ravier, S.; Cazaunau, M.; et al. Gaseous Products and Secondary Organic Aerosol Formation during Long Term Oxidation of Isoprene and Methacrolein. *Atmos. Chem. Phys.* **2015**, *15*, 2953−2968.
(33) Karl, M.; Dorn, H.-P.; Holland, F.; Koppmann, R.; Poppe, D.; Rupp, L.; Schaub, A.; Wahner, A. Product Study of the Reaction of OH Radicals with Isoprene in the Atmosphere Simulation Chamber SAPHIR. *J. Atmos. Chem.* **2006**, *55*, 167−187.
(34) Nguyen, T. B.; Roach, P. J.; Laskin, J.; Laskin, A.; Nizkorodov, S. A. Effect of Humidity on the Composition of Isoprene Photooxidation Secondary Organic Aerosol. *Atmos. Chem. Phys.* **2011**, *11*, 6931−6944.
(35) Crutzen, P. J.; Williams, J.; Pöschl, U.; Hoor, P.; Fischer, H.; Warneke, C.; Holzinger, R.; Hansel, A.; Lindinger, W.; Scheeren, B.; et al. High Spatial and Temporal Resolution Measurements of Primary Organics and their Oxidation Products over the Tropical Forests of Surinam. *Atmos. Environ.* **2000**, *34*, 1161−1165.
(36) Berndt, T. Formation of Carbonyls and Hydroperoxyenals (HPALDs) from the OH Radical Reaction of Isoprene for low-NOx Conditions: Influence of Temperature and Water Vapour Content. *J. Atmos. Chem.* **2012**, *69*, 253−272.
(37) Navarro, M. A.; Dusanter, S.; Hites, R. A.; Stevens, P. S. Radical Dependence of the Yields of Methacrolein and Methyl Vinyl Ketone from the OH-Initiated Oxidation of Isoprene under NO_x-Free Conditions. *Environ. Sci. Technol.* **2011**, *45*, 923−929.
(38) Lee, W.; Baasandorj, M.; Stevens, P. S.; Hites, R. A. Monitoring OH-Initiated Oxidation Kinetics of Isoprene and Its Products Using Online Mass Spectrometry. *Environ. Sci. Technol.* **2005**, *39*, 1030−1036.
(39) Navarro, M. A.; Dusanter, S.; Stevens, P. S. Temperature Dependence of the Yields of Methacrolein and Methyl Vinyl Ketone from the OH-Initiated Oxidation of Isoprene under NO_x-Free Conditions. *Atmos. Environ.* **2013**, *79*, 59−66.
(40) Liu, Y. J.; Herdlinger-Blatt, I.; McKinney, K. A.; Martin, S. T. Production of Methyl Vinyl Ketone and Methacrolein via the Hydroperoxyl Pathway of Isoprene Oxidation. *Atmos. Chem. Phys.* **2013**, *13*, 5715−5730.
(41) Bates, K. H.; Nguyen, T. B.; Teng, A. P.; Crounse, J. D.; Kjaergaard, H. G.; Stoltz, B. M.; Seinfeld, J. H.; Wennberg, P. O. Production and Fate of C-4 Dihydroxycarbonyl Compounds from Isoprene Oxidation. *J. Phys. Chem. A* **2016**, *120*, 106−117.
(42) Budisulistiorini, S. H.; Nenes, A.; Carlton, A. G.; Surratt, J. D.; McNeill, V. F.; Pye, H. O. T. Simulating Aqueous-Phase Isoprene-Epoxydiol (IEPOX) Secondary Organic Aerosol Production During the 2013 Southern Oxidant and Aerosol Study (SOAS). *Environ. Sci. Technol.* **2017**, *51*, 5026−5034.
(43) Hu, W. W.; Campuzano-Jost, P.; Palm, B. B.; Day, D. A.; Ortega, A. M.; Hayes, P. L.; Krechmer, J. E.; Chen, Q.; Kuwata, M.; Liu, Y. J.; et al. Characterization of a Real-Time Tracer for Isoprene Epoxydiols-Derived Secondary Organic Aerosol (IEPOX-SOA) from Aerosol Mass Spectrometer Measurements. *Atmos. Chem. Phys.* **2015**, *15*, 11807−11833.
(44) Wang, W.; Kourtchev, I.; Graham, B.; Cafmeyer, J.; Maenhaut, W.; Claeys, M. Characterization of Oxygenated Derivatives of Isoprene Related to 2-Methyltetrols in Amazonian Aerosols Using Trimethylsi-

DOI: 10.1021/acs.jpca.7b05879
J. Phys. Chem. A 2017, 121, 6460−6470

lylation and Gas Chromatography/Ion Trap Mass Spectrometry. *Rapid Commun. Mass Spectrom.* **2005**, *19*, 1343−1351.
(45) Riedel, T. P.; Lin, Y. H.; Zhang, Z.; Chu, K.; Thornton, J. A.; Vizuete, W.; Gold, A.; Surratt, J. D. Constraining Condensed-Phase Formation Kinetics of Secondary Organic Aerosol Components from Isoprene Epoxydiols. *Atmos. Chem. Phys.* **2016**, *16*, 1245−1254.
(46) Chung, S. H.; Seinfeld, J. H. Global Distribution and Climate Forcing of Carbonaceous Aerosols. *J. Geophys. Res.* **2002**, *107*, AAC 14−1−AAC 14−33.
(47) Lin, Y.-H.; Arashiro, M.; Martin, E.; Chen, Y.; Zhang, Z.; Sexton, K. G.; Gold, A.; Jaspers, I.; Fry, R. C.; Surratt, J. D. Isoprene-Derived Secondary Organic Aerosol Induces the Expression of Oxidative Stress Response Genes in Human Lung Cells. *Environ. Sci. Technol. Lett.* **2016**, *3*, 250−254.
(48) Eddingsaas, N. Formation of Low Vapor Pressure Compounds in Atmospheric Aerosols: Mechanism of Organosulfateformation. *Abstr. Pap. Am. Chem. Soc.* **2013**, *245*, 1.
(49) Froyd, K. D.; Murphy, S. M.; Murphy, D. M.; de Gouw, J. A.; Eddingsaas, N. C.; Wennberg, P. O. Contribution of Isoprene-Derived Organosulfates to Free Tropospheric Aerosol Mass. *Proc. Natl. Acad. Sci. U. S. A.* **2010**, *107*, 21360−21365.
(50) Pratt, K. A.; Fiddler, M. N.; Shepson, P. B.; Carlton, A. G.; Surratt, J. D. Organosulfates in Cloud Water above the Ozarks' Isoprene Source Region. *Atmos. Environ.* **2013**, *77*, 231−238.
(51) Shalamzari, M. S.; Ryabtsova, O.; Kahnt, A.; Vermeylen, R.; Herent, M. F.; Quetin-Leclercq, J.; Van der Veken, P.; Maenhaut, W.; Claeys, M. Mass Spectrometric Characterization of Organosulfates Related to Secondary Organic Aerosol from Isoprene. *Rapid Commun. Mass Spectrom.* **2013**, *27*, 784−794.
(52) Edney, E. O.; Kleindienst, T. E.; Jaoui, M.; Lewandowski, M.; Offenberg, J. H.; Wang, W.; Claeys, M. Formation of 2-Methyl Tetrols and 2-Methylglyceric Acid in Secondary Organic Aerosol from Laboratory Irradiated Isoprene/NO_X/SO_2/Air Mixtures and their Detection in Ambient PM2.5 Samples Collected in the Eastern United States. *Atmos. Environ.* **2005**, *39*, 5281−5289.
(53) Nguyen, T. B.; Crounse, J. D.; Teng, A. P.; St. Clair, J. M.; Paulot, F.; Wolfe, G. M.; Wennberg, P. O. Rapid Deposition of Oxidized Biogenic Compounds to a Temperate Forest. *Proc. Natl. Acad. Sci. U. S. A.* **2015**, *112*, E392−E401.
(54) *Estimation Programs Interface Suite for Microsoft Windows*, 4.11; United States Environmental Protection Agency: Washington, DC, 2012.
(55) *HenryWin*, 3.20; United States Environmental Protection Agency: Washington, DC, 2011.
(56) Compernolle, S.; Ceulemans, K.; Müller, J. F. EVAPORATION: a New Vapour Pressure Estimation Method for Organic Molecules Including Non-Additivity and Intramolecular Interactions. *Atmos. Chem. Phys.* **2011**, *11*, 9431−9450.
(57) Herrmann, H. Kinetics of Aqueous Phase Reactions Relevant for Atmospheric Chemistry. *Chem. Rev.* **2003**, *103*, 4691−4716.
(58) Schaefer, T.; Schindelka, J.; Hoffmann, D.; Herrmann, H. Laboratory Kinetic and Mechanistic Studies on the OH-Initiated Oxidation of Acetone in Aqueous Solution. *J. Phys. Chem. A* **2012**, *116*, 6317−6326.
(59) Chin, M.; Wine, P. H. A Temperature-Dependent Kinetics Study of the Aqueous Phase Reactions OH + SCN^- → $SCNOH^-$ and SCN + SCN^- ⇆ $(SCN)_2^-$. *J. Photochem. Photobiol., A* **1992**, *69*, 17−25.
(60) Herrmann, H.; Hoffmann, D.; Schaefer, T.; Bräuer, P.; Tilgner, A. Tropospheric Aqueous-Phase Free-Radical Chemistry: Radical Sources, Spectra, Reaction Kinetics and Prediction Tools. *ChemPhysChem* **2010**, *11*, 3796−3822.
(61) White, J. U. Long Optical Paths of Large Aperture. *J. Opt. Soc. Am.* **1942**, *32*, 285−288.
(62) Gaillard de Semainville, P.; Hoffmann, D.; George, C.; Herrmann, H. Study of Nitrate Radical (NO_3) Reactions with Carbonyls and Acids in Aqueous Solution as a Function of Temperature. *Phys. Chem. Chem. Phys.* **2007**, *9*, 958−968.
(63) Hoffmann, D.; Weigert, B.; Barzaghi, P.; Herrmann, H. Reactivity of Poly-Alcohols towards OH, NO_3 and SO_4^- in Aqueous Solution. *Phys. Chem. Chem. Phys.* **2009**, *11*, 9351−9363.
(64) Gligorovski, S. *Laser Based Studies of OH Radical Reactions in Aqueous Solution*; Universität Leipzig: Leipzig, 2005.
(65) Hesper, J. *Spektroskopische und Kinetische Untersuchungen von Reaktionen der Radikale O_2^- und OH in Wässriger Phase*; Universität Leipzig: Leipzig, 2003.
(66) Schöne, L.; Schindelka, J.; Szeremeta, E.; Schaefer, T.; Hoffmann, D.; Rudzinski, K. J.; Szmigielski, R.; Herrmann, H. Atmospheric Aqueous Phase Radical Chemistry of the Isoprene Oxidation Products Methacrolein, Methyl Vinyl Ketone, Methacrylic Acid and Acrylic Acid - Kinetics and Product Studies. *Phys. Chem. Chem. Phys.* **2014**, *16*, 6257−6272.
(67) Smoluchowski, M. v. Versuch einer Mathematischen Theorie der Koagulationskinetik Kolloider Lösungen. *Z. Phys. Chem.* **1918**, *92*, 129.
(68) Wilke, C. R.; Chang, P. Correlation of Diffusion Coefficients in Dilute Solutions. *AIChE J.* **1955**, *1*, 264−270.
(69) Crittenden, J. C.; Trussell, R. R.; Hand, D. W.; Howe, K. J.; Tchobanoglous, G., Appendix C: Physical Properties of Water. In *MWH's Water Treatment: Principles and Design*, 3rd ed.; John Wiley & Sons, Inc.: New York, 2012; pp 1861−1862.
(70) Kojima, H.; Bard, A. J. Determination of Rate Constants for the Electroreduction of Aromatic Compounds and their Correlation with Homogeneous Electron Transfer Rates. *J. Am. Chem. Soc.* **1975**, *97*, 6317−6324.
(71) Joback, K. G.; Reid, R. C. Estimation of Pure-Component Properties from Group-Contributions. *Chem. Eng. Commun.* **1987**, *57*, 233−243.
(72) Monod, A.; Doussin, J. F. Structure-Activity Relationship for the Estimation of OH-Oxidation Rate Constants of Aliphatic Organic Compounds in the Aqueous Phase: Alkanes, Alcohols, Organic Acids and Bases. *Atmos. Environ.* **2008**, *42*, 7611−7622.
(73) Doussin, J. F.; Monod, A. Structure−Activity Relationship for the Estimation of OH-Oxidation Rate Constants of Carbonyl Compounds in the Aqueous Phase. *Atmos. Chem. Phys.* **2013**, *13*, 11625−11641.
(74) Schöne, L.; Herrmann, H. Kinetic Measurements of the Reactivity of Hydrogen Peroxide and Ozone towards Small Atmospherically Relevant Aldehydes, Ketones and Organic Acids in Aqueous Solutions. *Atmos. Chem. Phys.* **2014**, *14*, 4503−4514.
(75) Stefan, M. I.; Bolton, J. R. Reinvestigation of the Acetone Degradation Mechanism in Dilute Aqueous Solution by the UV/H_2O_2 Process. *Environ. Sci. Technol.* **1999**, *33*, 870−873.
(76) Eugene, A. J.; Guzman, M. I. Reactivity of Ketyl and Acetyl Radicals from Direct Solar Actinic Photolysis of Aqueous Pyruvic Acid. *J. Phys. Chem. A* **2017**, *121*, 2924−2935.
(77) Eugene, A. J.; Xia, S.-S.; Guzman, M. I. Aqueous Photochemistry of Glyoxylic Acid. *J. Phys. Chem. A* **2016**, *120*, 3817−3826.
(78) Raventos-Duran, T.; Camredon, M.; Valorso, R.; Mouchel-Vallon, C.; Aumont, B. Structure-Activity Relationships to Estimate the Effective Henry's Law Constants of Organics of Atmospheric Interest. *Atmos. Chem. Phys.* **2010**, *10*, 7643−7654.
(79) Angyal, S. J. The Lobry de Bruyn-Alberda van Ekenstein Transformation and Related Reactions. In *Glycoscience: Epimerisation, Isomerisation and Rearrangement Reactions of Carbohydrates*; Stütz, A. E., Ed.; Springer Berlin Heidelberg: Berlin, Heidelberg, 2001; pp 1−14.
(80) Schaefer, T.; van Pinxteren, D.; Herrmann, H. Multiphase Chemistry of Glyoxal: Revised Kinetics of the Alkyl Radical Reaction with Molecular Oxygen and the Reaction of Glyoxal with OH, NO_3, and SO_4^- in Aqueous Solution. *Environ. Sci. Technol.* **2015**, *49*, 343−350.
(81) Hesse, G.; Stahl, H. Methylredukton. *Chem. Ber.* **1956**, *89*, 2424−2429.

DOI: 10.1021/acs.jpca.7b05879
J. Phys. Chem. A 2017, 121, 6460−6470